Dynamic Behavior in Ternary Polymer Solutions. Polyisobutylene in Chloroform Studied Using Dynamic Light Scattering and Pulsed Field Gradient NMR

Wyn Brown* and Pu Zhou

Institute of Physical Chemistry, University of Uppsala, Box 532, 751 21 Uppsala, Sweden.
Received January 26, 1989

ABSTRACT: Measurements of translational diffusion in ternary systems have been made using dynamic light scattering (DLS) on the homopolymeric polyisobutylene (PIB) system: PIB_1/PIB_2/chloroform. Since the signal from one polymer is modulated by the second, one obtains a bimodal autocorrelation function. The two modes correspond to the cooperative diffusion coefficient of the semidilute matrix polymer and, at a trace concentration of the probe polymer, the self-diffusion coefficient of the latter. Using the independent method pulsed field gradient NMR, the respective components were confirmed in the DLS decay time spectrum obtained by Laplace inversion. The experiments using this approach for determining self-diffusion coefficients in ternary systems encompass two main aspects: (i) The diffusion of a high molecular weight PIB probe in semidilute solutions of PIB of lower molecular weight. The chain moves through the viscous medium by a Stokes–Einstein mechanism, and the reduced diffusion coefficient of the coil is identical with that for a hard sphere measured in the same matrix solutions. It is found that for a given probe $D_{probe} \sim M_{matrix}^{-0.55}$. There is possibly a coupling between the network and self-diffusion modes (for both chain and hard sphere) at higher network concentrations. Comparisons with data for polystyrene (PS) show that the PS coil is substantially more contracted than the PIB coil in the same PIB matrix, illustrating the influence of chain incompatibility. (ii) The translation of low molecular weight PIB fractions in a semidilute network of a high molecular weight PIB fraction. The concentration dependence of the probe diffusion coeficient is best described by a smooth curve, although within a limited range of concentration the data are not inconsistent with the scaling prediction for self-diffusion: $D \sim C^{-1.75}M^{-2}$. At the highest concentrations an increasing dependence of D_{probe} on concentration is noted. A model in which the diffusional mobility is determined by the increasing congestion as the entanglement density in the matrix increases is seen to be as plausible as reptation.

Introduction

The self-diffusion of polymer chains in semidilute solution is of considerable interest. Experimental methods used include forced Rayleigh scattering (FRS), and pulsed-field-gradient NMR (PFG NMR). An alternative approach is to make dynamic light scattering (DLS) measurements on ternary polymer solutions using the optical labeling method (see, for example, ref 1–11). In the latter, a solvent is selected that is isorefractive with polymer A, while polymer B has a significant contrast such that accurate DLS measurements can be made using a relatively low concentration of this component. In this way the translational diffusion of B in semidilute solutions of A has been examined in a variety of systems. It is usually assumed that the necessarily nonzero concentration of B is close to the infinite dilution value so that its self-diffusion coefficient is determined; Chang et al.[11] have established that this is probably justifiable. A source of complication, nevertheless, can be an incomplete refractive index matching of the solvent with A, leading to "contamination" of the correlation function for polymer B. Chu et al.[7,8] circumvented this by adjusting the temperature. More serious, however, is the degree to which the "invisible" polymer component potentially influences the dynamics of the observed polymer, by, for example, changing its dimensions. Lodge and co-workers[5] demonstrated that the polystyrene coil (PS) contracts to close to its Θ dimensions in dilute PVME solutions, even though these two polymers are conceived macroscopically to be completely compatible. To obviate this problem we have chosen an alternative approach and using DLS have examined the homopolymeric system, in which polymers A and B are chemically identical, differing only in molecular weight. Phillies[12] and Pusey et al.[13] have treated the special case of interacting spherical particles where the two scattering species are identical except in size. Phillies[14] subsequently dealt with the system in which the scattering is dominated by a species of vanishingly low concentration and showed that the self-diffusion coefficient of this component may be derived. More recently, Joanny et al.[15] considered the thermodynamics of such systems and the implications for scaling.

Using the random-phase approximation technique, Benmouna et al.[16,17] considered the general case of two polymers in a good solvent and showed that the correlation function of the scattered intensity is a sum of two exponential functions, where the relaxation rates (Γ_C and Γ_I) characterizing the two diffusive components are termed the cooperative and interdiffusion modes, respectively. The former is the collective diffusion coefficient of the polymer above the overlap concentration (C^*),[37] and the latter refers to the motion of individual chains with respect to each other and becomes equal to the self-diffusion coefficient at sufficiently low concentrations. These authors concluded that in order to observe both modes the relative amplitudes should be approximately equal and the decay rates sufficiently different for separation. Recent developments in wide band autocorrelators in conjunction with new methods of extracting decay time distributions by, for example, Laplace inversion using a modified form of CONTIN[19] suitable for extended ranges of decay times or using the maximum entropy method, MAXENT,[20,21] make it possible to substantially relax these conditions. Relaxation rates may now be evaluated with good precision if the noise level is low even for very small relative amounts (a few percent) of one polymer in solutions of the other, and thus one may derive its self-diffusion coefficient. Thus we have a different approach to determining self-diffusion coefficients in semidilute solution, which complements PFG NMR and FRS. Since decay times covering a range of up to 8 decades on the time scale are accessible in a single experiment, the span of relative molecular weights is correspondingly wide and permits one to examine the two main cases of interest: i.e., trace amounts of a large coil in both dilute and semidilute solutions of the smaller component as well as the converse of a small chain in semidilute solutions of the larger species. (Obviously, there will be an inaccessible molecular weight range over which,

0024-9297/89/2222-4031$01.50/0

as the molecular weights approach each other, the two species are insufficiently resolved. Also, it is not possible to measure the molecular dimensions of the components using static light scattering when they possess the same refractive index increment.) The present polyisobutylene system, PIB_1/PIB_2/deuteriated chloroform ($CDCl_3$), was chosen since, apart from the availability of sharp fractions of widely different molecular weight, this polymer has a strong, well-defined proton signal well-suited to pulsed field gradient NMR measurements. Thus self-diffusion measurements could also be made employing this independent technique and used to verify the peak assignments made in the DLS decay time distributions under various conditions.

Another aspect that is examined is a comparison of the self-diffusion of a high molecular weight PS fraction in the same PIB fractions as used above in order to examine the influence of a limited polymer compatibility on the transport process.

Experimental Section

Polyisobutylene (PIB) samples were in part narrow-distribution fractions obtained from Polymer Standards Service, Mainz, FRG. The molecular weights, polydispersity indices, and intrinsic viscosities were summarized in ref 10. Polystyrenes (PS) were from Toya Soda, Ltd., Tokyo, Japan [$M_w = 8 \times 10^6$ (M_w/M_n = 1.05)] and Polymer Standards, Ltd., Pittsburgh, PA [$M_w = 9.3 \times 10^5$, $M_w/M_n = 1.03$; $M_w = 3 \times 10^5$, $M_w/M_n = 1.04$].

Sterically stabilized silica particles were kindly provided by Dr. K. de Kruif, University of Utrecht, The Netherlands. The synthesis was earlier described by Vrij et al.,[22] the stabilizing layer being terminally grafted $C_{18}H_{37}OSi$. The hydrodynamic radius of the spheres is 1595 Å, determined by DLS in chloroform. Solvents used were spectroscopic grade from Merck, Darmstadt, FRG.

Pulsed field gradient NMR measurements were made on protons at 99.6 MHz with a standard JEOL FX-100 Fourier transform NMR spectrometer as described in ref 23. An internal deuterium lock ($CDCl_3$) was used for field frequency stabilization. The time between the 90° and 180° radio frequency pulses was 140 ms for all durations of the gradient pulses of constant field strength. The experimental uncertainty in the diffusion coefficient is about ±1.5% at a value of 1×10^{-11} m^2 s^{-1}.

Dynamic Light Scattering. Measurements were made as previously described.[24] Stock solutions of the probe chains were initially prepared, and these were used as the solvent for preparing the semidilute solutions of the matrix polymer. Dilutions were made using the same solvent solution. All solutions were filtered using 0.45-μm Millipore filters (Millex, Durapore). Equilibration was for a few days, following filtration and prior to measurements. All determinations were made at 25 °C and initially over a wide range of angles to ascertain q^2 dependence for the matrix and probe relaxation rates. Subsequent measurements were made at $\theta = 20°$.

The autocorrelator was a multi-τ model from ALV, Langen, FRG, employing 23 simultaneous sampling times and allowing a monitoring of very widely spaced decays in the same experiment. Laplace transformation $(g_{(1)}(t) = \int_0^\infty A(\tau) \exp(-t/\tau)\, d\tau)$ of the correlation curves $g_{(1)}(t)$ was performed using either MAXENT or a constrained regularization calculation REPES[18] to obtain the distribution $A(\tau)$ of decay times. The algorithm differs in a major respect from CONTIN developed by Provencher[19] in that the relevant computer program directly minimizes the sum of the squared differences between the experimental and calculated $g_{(2)}(t)$ functions ($g_{(2)}(t) = g^2_{(1)}(t)$) using nonlinear programming and the a priori chosen parameter "probability to reject" P (usually with $P = 0.5$). The analysis of data, encompassing 191 exponentially spaced points and a grid density of typically 10 per decade in time, may be made on-line with an IBM-AT computer in a few minutes. It was found that the decay time distributions were closely similar to those obtained using MAXENT.[20,21] The latter analysis was, however, more time consuming and does not, at least in its presently used form, allow comparisons of different degrees of smoothing.

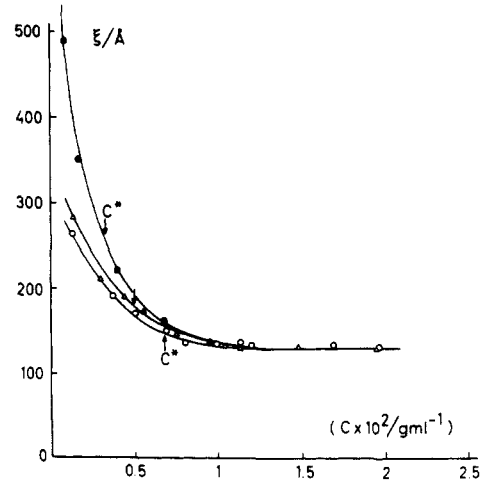

Figure 1. Concentration dependence of the dynamic correlation length for various molecular weights of poly(isobutylene) in chloroform: (●) 4.9×10^6; (△) 1.9×10^6; (○) 1.1×10^6. Overlap concentrations evaluated according to footnote 37 are indicated.

Viscosity measurements were made using an Ubbelohde capillary viscometer at 25 °C.

Results and Discussion

1. Large Coil in Solutions of Smaller Coils. The present measurements were made at an angle of $\theta = 20°$ at which the inequality $qR_g < 1$ is valid for the probe polymer. In this case the internal modes of the single coil will not make a significant contribution to the correlation function. The semidilute solution used for the matrix component, on the other hand, is characterized by the cooperative diffusion coefficient (D_C), which is inversely proportional to the dynamic correlation length, ξ, defined by:

$$D_C = kT/6\pi\eta_0\xi \qquad (1)$$

At the angle of 20°, $q\xi < 1$ in the semidilute region for the PIB matrix and the blob of size ξ will dominate the structure factor. (With the largest mesh sizes and at high measurement angles such that $q\xi > 1$, it may also, in principle, be possible to resolve the internal modes for the entangled chains.) In the present experiments the concentration range used for the matrix polymer spans the dilute to modest semidilute range.

Figure 1 shows the concentration dependence of the dynamic correlation length for PIB matrix chains of various molecular weights calculated from the diffusion coefficients determined in the absence of the large PIB probe chains. A molecular weight independent length does not result until concentrations substantially exceed coil overlap. The latter has been estimated for present purposes using the relationship $C^* = 1/[\eta]$, as in the previous communication.[10]

Figure 2 shows decay time distributions obtained using the maximum entropy method (MAXENT) for PIB (4.9×10^6) in solutions of PIB with molecular weight $M = 6.1 \times 10^5$. The two peaks are well-defined since the molecular weights differ sufficiently, and they do not overlap at any concentration. The relaxation frequencies are given in the output of the MAXENT program. Diffusion coefficients were evaluated as $D = (\Gamma/q^2)_{q\to 0}$, since both peaks correspond to q^2 dependent processes (see Figure 3). It has, however, been amply demonstrated in earlier reports[24] that several dynamic processes may be observable in semidilute solutions; these range from the translational diffusion of the single coil in the vicinity of C^*, as well as a spectrum of internal modes of the entangled structure, to the move-

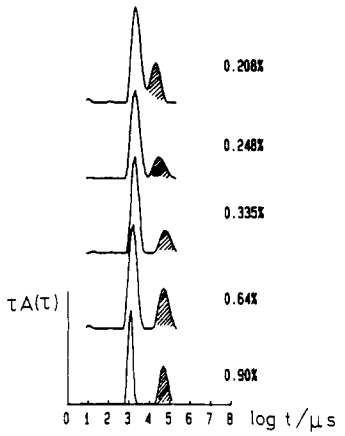

Figure 2. Decay-time distributions obtained using a modified form of CONTIN[18,19] for the ternary system: PIB(4.9×10^6) probe/PIB(2.47×10^5) matrix in chloroform at the concentrations shown. The shaded peaks represent the high MW probe. The quantity $\tau A(\tau)$ is shown plotted to give an equal area representation.

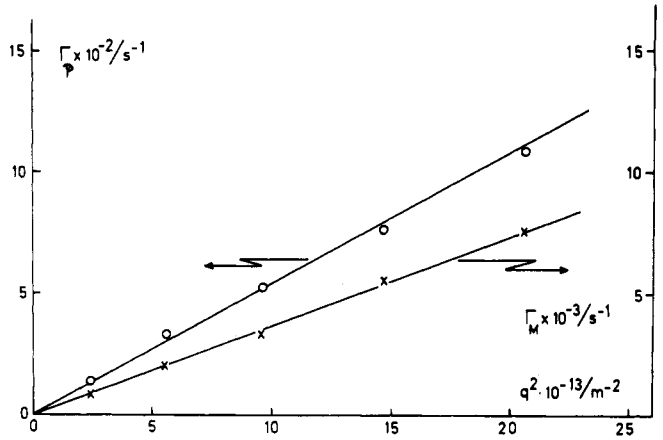

Figure 3. Relaxation rates for probe (O) and matrix (×) as a function of q^2 for the system shown in Figure 2 and at a matrix concentration of 0.64%. Diffusion coefficients from pulsed field gradient NMR (×) are included for the matrix polymer PIB ($M = 2.47 \times 10^5$).

ment of clusters of chains within the network, which becomes observable due to the size heterogeneity. We are concerned in the present paper with an intermediate concentration range where both the translational (interdiffusion) and cooperative motions may both be expected to contribute to the dynamic structure factor. We note that bimodal correlation functions have previously been observed in ternary systems in which the matrix component is refractive index matched to the solvent.[3,7,8] It was suggested there that the fast component could derive from a coupling of the motions of the probe with those of the semidilute matrix. This case has, however, also been treated by Benmouna et al.[16] who show that a bimodal autocorrelation function must result in such systems. That the fast peak in the distributions of Figure 2 derives from the lower molecular weight component is shown by (a) extrapolation of the corresponding diffusion coefficient to infinite dilution where it coincides with the value determined by extrapolation of dilute solution data for the binary system, and (b) the coincidence of the infinite dilution value with that obtained using the data from pulsed field gradient NMR. These data are shown for one of the fractions in Figure 4. A similar approach has been used to confirm the identification of the slow peak. It is also shown (see below, Figure 11) that the diffusion coefficients for the probe chain are identical with the self-diffusion

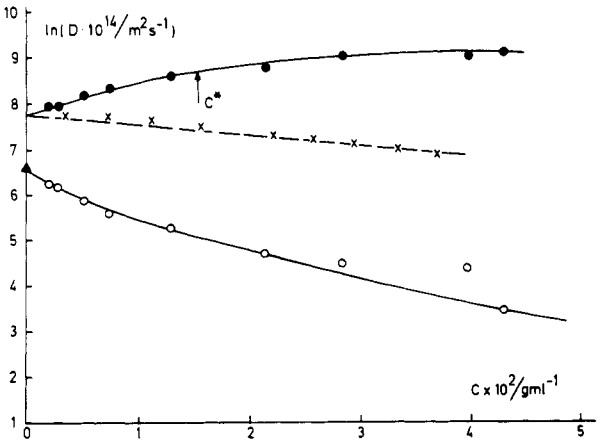

Figure 4. Diffusion coefficients for probe (O) and for matrix (●) for the system of Figure 2, where the diffusion coefficients have been evaluated from the moments of the peaks. Diffusion coefficients from pulsed field gradient NMR (×) are included for the matrix polymer PIB ($M = 2.47 \times 10^5$).

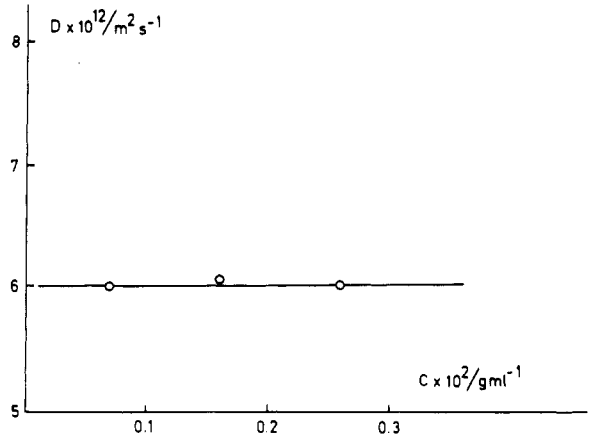

Figure 5. Diffusion coefficients for the probe polymer PIB ($M = 4.9 \times 10^6$) as a function of its concentration. Concentration of matrix polymer PIB ($M = 2.47 \times 10^5$) = 0.19%.

coefficients determined by PFG NMR at finite concentrations over the concentration range used.

The present measurements were made in the range of matrix polymer concentration up to about $3\text{–}5C^*$, depending on the molecular weight of the short chains. This upper limit in concentration was imposed by the very low diffusion coefficients found for the probe chain (D_{probe}), which decrease to about 5×10^{-14} m^2 s^{-1} ($\approx$3% of the value at infinite dilution) at the highest matrix concentration and also by the very low relative amplitude of the probe component.

In a semidilute solution of shorter chains, a large coil is expected to move by Stokes–Einstein diffusion, i.e. at a rate determined by the macroscopic viscosity of the medium since the smaller chains will disentangle in a time that is much shorter than the relaxation time characterizing translation of the large probe coil. The disentanglement time (T_R) may be estimated in good solvents from the relationship given by de Gennes:[25]

$$T_R = (6\pi\eta_0/kT)R_g^3(C/C^*)^{1.5} \quad (2)$$

As an example, with the probe of $M = 4.9 \times 10^6$ and with the matrix $M = 2.47 \times 10^5$ at a concentration of $2C^*$, we have $(T_R)_{matrix} = 1.46 \times 10^{-4}$ s using eq 2 while the relaxation time for the probe ($\tau_{probe} \approx (Dq^2)^{-1}_{\theta=20°}$) is 6.3×10^{-2} s at this concentration. Figure 5 shows data obtained when the concentration of the probe is varied, holding the matrix polymer concentration fixed. There is no significant de-

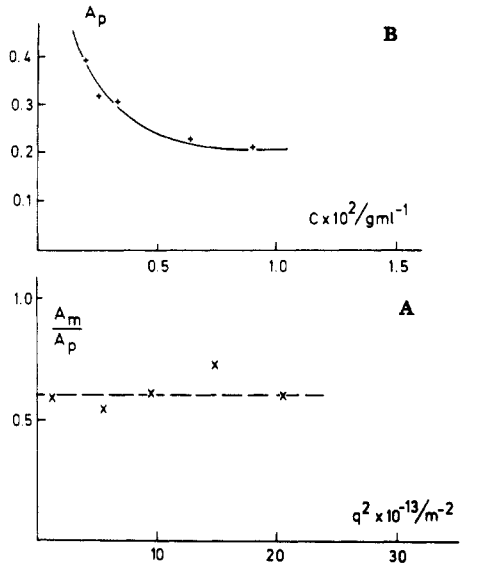

Figure 6. (A) Ratio of relative amplitudes (A_m/A_p) as a function of q^2 for the system shown in Figures 2 and 3 (probe = 4.9×10^6; matrix = 2.47×10^5). The matrix concentration is 0.19%. (B) Dependence of the relative amplitude of the probe, A_p, on the total concentration of polymer system as in Figures 2 and 3 ($C^* \simeq 1.5\%$).

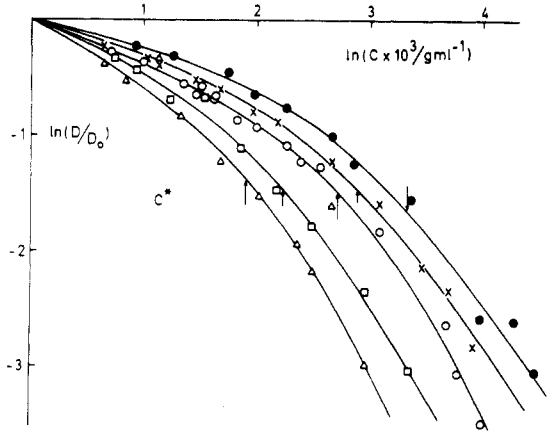

Figure 7. Logarithmic diagram relating D/D_0 and matrix concentration for the PIB ($M = 4.9 \times 10^6$) probe in PIB fractions of the following molecular weights: 8.04×10^4 (●), 1.82×10^5 (×), 2.47×10^5 (○), 6.1×10^5 (□), 1.1×10^6 (△).

pendence of D_{probe} on probe concentration, showing that in this system its self-diffusion coefficient is determined at finite concentrations. We note that, with chemically different polymers, increasing the matrix concentration may lead to a negative dependence (since the solvent quality is in effect reduced); Chang et al.[11] have, however, shown this dependence to be small.

Figure 6A shows the dependence of the ratio of relative amplitudes, A_m/A_p, on the square of the scattering vector, the values of which have been obtained from the moments of the peaks in the MAXENT decay time distributions. The angular dependence is insignificant. This is in agreement with the results of static light scattering measurements made as a function of angle, in which the reduced scattering intensity function, KC/R_θ is observed to be angle independent.

Figure 6B illustrates the dependence of the amplitude of the probe polymer, A_p, on the total polymer concentration. The amplitudes of the two components are complicated functions of the composition. This curve follows the trend predicted by Benmouna et al.[16]

Figure 7 shows a double logarithmic plot of the reduced diffusion coefficient, where D was evaluated from the

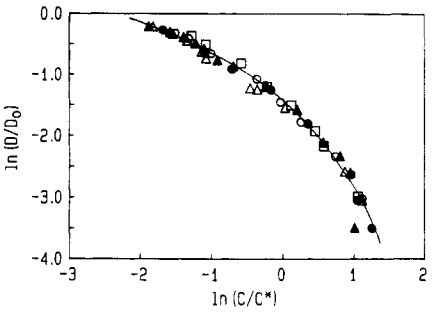

Figure 8. Data in Figure 7 where the matrix concentrations have been normalized by C^* for the PIB fractions: 8.04×10^4 (△), 1.82×10^5 (▲), 2.47×10^5 (●), 6.1×10^5 (○), 1.1×10^6 (□).

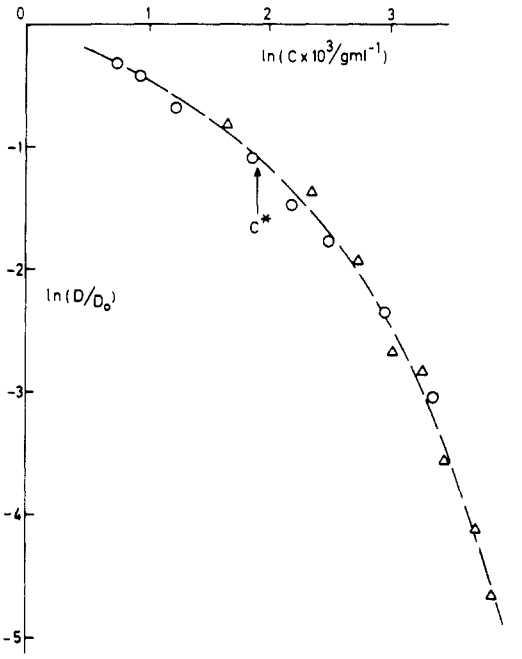

Figure 9. Comparison of reduced diffusion coefficients for (i) PIB (4.9×10^6; R_g = 1400 Å) in PIB (6.1×10^5) (△) and (ii) SiO_2 spheres (R_H = 1595 Å) in PIB (6.1×10^5) (○). The overlap concentration indicated is for the matrix polymer.

moments of the peaks (for example, those illustrated in Figure 2) for the probe polymer ($M = 4.9 \times 10^6$) versus concentration of the matrix polymer for a series of lower molecular weight fractions of the latter ranging from 8×10^4 to 1.1×10^6. D_0 was obtained as the infinite dilution intercept in the binary system: probe/solvent. When the matrix concentration is normalized using C^*, the data fall on a universal curve as illustrated in Figure 8. This behavior is anticipated from scaling theory[25,26] and was previously demonstrated for stearic acid coated SiO_2 spheres in the same PIB solutions[10] and also for polystyrene chains in semidilute PMMA solutions.[9] Thus $D_{probe} \sim M_{matrix}^{-0.55}$ (since $C^* \sim M^{-0.55}$).

Figure 9 compares the normalized translational diffusion coefficients for the PIB probe chain ($M = 4.9 \times 10^6$) with the previously determined values for stearic acid coated hard spheres (R_H = 1595 Å). The data fall on a common curve within experimental error and demonstrate that, to a first approximation, a simple Stokes–Einstein diffusion is the mechanism followed by both the hard sphere and the random coil and that the coil is indistinguishable from a hard sphere in such an experiment.

The change in expansion of a long chain immersed in a solution of shorter chains, which might be expected to influence the form of the curves in Figure 7, was considered by de Gennes[25] and subsequently by Joanny et al.[28] Due

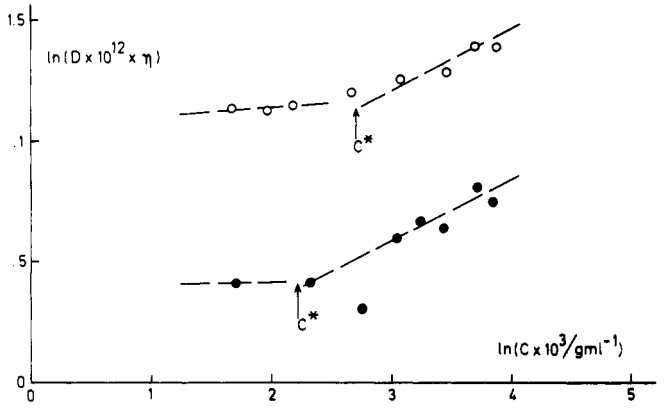

Figure 10. Dependence of the product ($D_{probe}\eta$) on concentration for the systems: (A) PIB (4.9×10^6) in PIB (2.47×10^5 (○)); (B) SiO_2 spheres in PIB (6.1×10^5 (●)). The slope above C^* is 0.25.

to the screening of the excluded volume interactions, which should be more effective when the surrounding chains are shorter than the test chain, the coil radius was predicted to decrease as $C^{-0.25}$. This may be tested by plotting the product ($D_{probe}\eta$), which should scale as the hydrodynamic radius, versus C in a log–log diagram, where η is the experimental bulk viscosity of the solutions. Such a curve is depicted in Figure 10A, where above $C = C^*$ the broken line has been inserted with a slope of 0.25. Surprisingly, however, Figure 10B shows that a similar pattern is also found for the hard sphere. Thus, we conclude that, as the average mesh size of the matrix decreases with increasing concentration and the matrix becomes entangled, there is probably an increased coupling of the motions of probe particle and network. Such an interpretation was, for example, suggested by Nemoto et al.[3] to explain the observed bimodal correlation function for the probe polymer, even when the semidilute matrix polymer was matched in refractive index to the solvent. Reina et al.[27] have also observed that, in the extreme case of highly cross-linked gels, a latex particle probe becomes trapped in the network, effectively labeling it and thereby reflecting the dynamics of the blob characterizing the matrix. The similarity between the data for coil and sphere in Figure 9 shows that deswelling effects on the coil must be negligible, contrary to the predictions of Joanny et al.[28] and the apparently supporting observation recently made by Léger.[29] A coupling of motions may also explain the observed enhancement of the self-diffusion[29] when the size of the probe chain is commensurate with that of the matrix.

Figure 11 shows a comparison of the concentration dependence of the self-diffusion coefficient from PFG NMR for $M = 4.9 \times 10^6$ with the DLS data for the same fraction when used as a probe in the matrix of $M = 6.1 \times 10^5$. The reduced concentration, C/C^*, has been plotted to remove the molecular weight dependence of D/D_0, which was established in Figure 7. The agreement between the data sets confirms that the quantity determined in DLS experiments corresponds to the self-diffusion coefficient for the probe chain.

2. Smaller Chains in Solutions of Larger Coils. The reverse experiment of using the smaller coils at trace concentrations as the probe polymer, diffusing in dilute and semidilute solutions of the larger chains, is of necessity a more difficult experiment since the scattering of the smaller species is lower. Nevertheless, this line is worth pursuing since, with a judicious choice of relative molecular weights, it potentially sheds light on a possible S–E diffusion/reptation crossover. A similar approach using FRS has recently been reported by Marmonier and Léger.[30] Figure 12 summarizes the data obtained in the PIB(M =

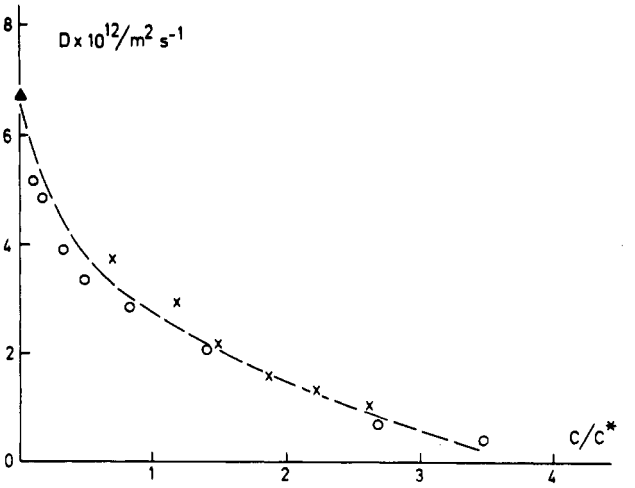

Figure 11. Comparison of the concentration dependence of the self-diffusion coefficients for PIB (4.9×10^6) determined as follows: (i) self-diffusion measurements in the binary system using PFG NMR (×), (ii) using dynamic light scattering in PIB ($M = 6.1 \times 10^5$) as the matrix (○). The concentrations are expressed as C/C^* in order to remove the matrix molecular weight dependence (compare Figures 7 and 8).

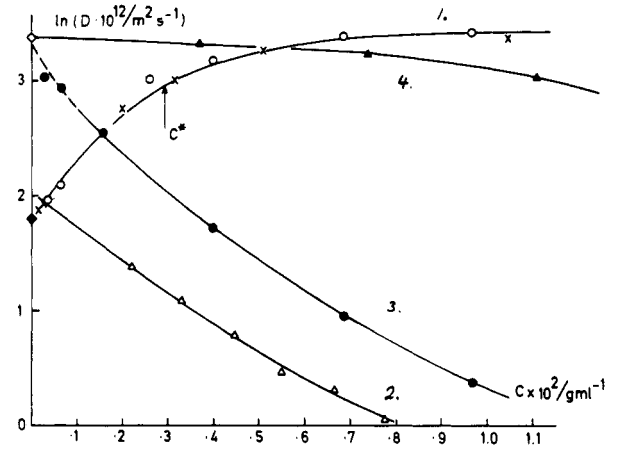

Figure 12. Data for PIB (4.9×10^6) as matrix in PIB (2.47×10^5) as probe: (1) 4.9×10^6 in the ternary system (○), DLS measurements; 4.9×10^6 in binary system (×) DLS; (2) 4.9×10^6 binary system (△), PFG NMR; (3) 2.47×10^5 ternary system (●), DLS; (4) 2.47×10^5 binary system (▲), PFG NMR. (The points at $C = 0$ are extrapolated values from measurements in highly dilute binary solutions of each fraction.)

2.47×10^5)/PIB($M = 4.9 \times 10^6$)/$CDCl_3$ system, curves being shown for both molecular weight species in this diagram. The radius of gyration, R_g, for $M = 2.47 \times 10^5$ is about 275 Å,[10] which exceeds the dynamic correlation length of the $M = 4.9 \times 10^6$ matrix ($\xi = 175$ Å at $C = C^*$ and $\xi = 128$ Å at $C = 3C^*$, see Figure 1). The smaller chains should thus be constrained to reptate at $C > C^*$ if this is the preferred mechanism for translation in congested systems. The matrix disentanglement time (calculated using eq 2) is longer than the probe relaxation time at all concentrations ($\tau_{probe} \approx (Dq^2)^{-1}_{\theta=20°}$).

Above the overlap concentration, the matrix component ($M = 4.9 \times 10^6$) is observed as the faster mode in the DLS experiment (curve 1), where the collective diffusion coefficient has been evaluated by MAXENT analysis of the correlation function. Included on curve 1 are points from DLS measurements on the binary system. Curve 2 represents self-diffusion coefficients for the same fraction determined in the binary solution by PFG NMR. The two curves have approximately the same intercept as $C \to 0$. Curve 3 shows the slow mode in the DLS experiment for the probe ($M = 2.47 \times 10^5$) and curve 4 the self-diffusion

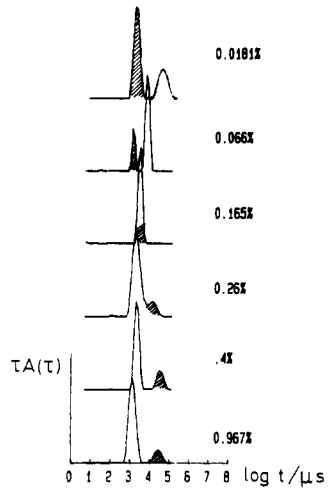

Figure 13. Decay-time distributions obtained by Laplace inversion using a modified form of CONTIN for the system shown in Figure 12. The shaded peaks represent the low MW probe. The concentrations are for the matrix polymer ($M = 4.9 \times 10^6$). The peaks at $C = 0.165\%$ superimpose as indicated at the crossing point between the probe and matrix curves for DLS measurements in Figure 12.

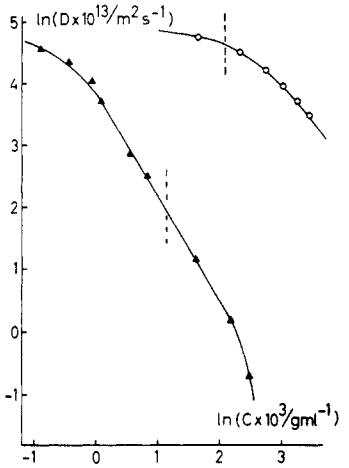

Figure 14. Logarithmic diagram of self-diffusion concentration dependence for PIB ($M = 8.56 \times 10^5$) in chloroform using: (a) pulsed field gradient NMR, in the binary system (○); (b) dynamic light scattering, in PIB matrix of $M = 4.9 \times 10^6$ (△). A tangent to curve a would have the value −1.3 at the higher concentrations; in b the major portion, which is approximately linear, has a slope of about −1.75. The vertical dotted lines indicate C^* for the matrix chains.

for this fraction obtained using PFG NMR in the binary solution. The points at $C = 0$ (diamonds) were obtained by extrapolation of DLS data for dilute binary solutions of each polymer fraction. It is noted that the matrix and probe data cross at a concentration of about 0.165×10^{-2} g mL^{-1}. The crossover is clearly seen in the decay-time spectra illustrated in Figure 13 where only a single peak is observable at this concentration in the spectrum. Thus, by utilizing this combination of methods it is possible to unambiguously identify the contributions from the two molecular weight fractions.

Figure 14 compares the data sets with matrix molecular weight (MW) (a) much larger than the probe and (b) identical with that of the probe. Figure 14 shows that (i) the dependence of the probe self-diffusion coefficient on the MW of the matrix polymer is significant and (ii) the predicted $D \sim M^{-2}C^{-1.75}$ relationship is obeyed over a limited range of concentration, as might be expected only when $(T_R)_{matrix} \gg (\tau)_{probe}$. When this is so, the theoretical slope is observed even when $C < C^*$ as defined here.[37] This

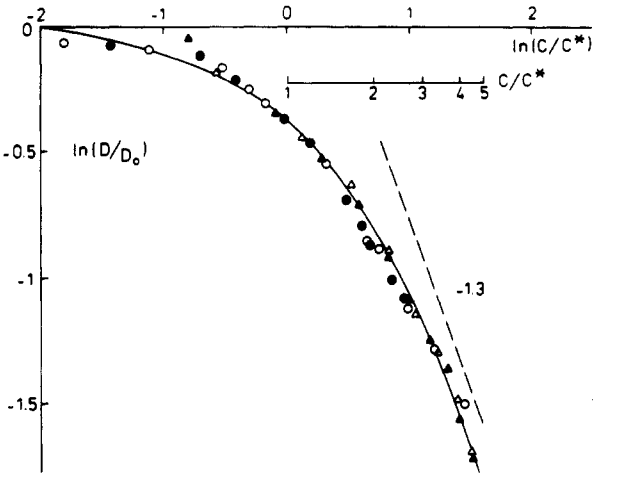

Figure 15. Logarithmic plot of the reduced diffusion coefficient, D/D_0, from PFG NMR measurements versus the reduced concentration, C/C^*, for PIB fractions in chloroform: (○) 1.82×10^5; (●) 2.47×10^5; (△) 6.51×10^5; (▲) 8.56×10^5. The asymptotic slope is about −1.3.

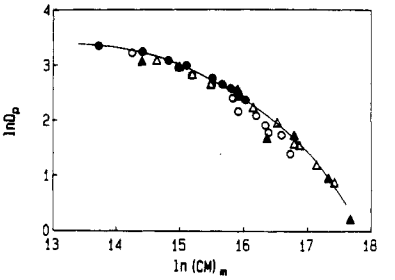

Figure 16. Plots of ln D_{probe} versus ln CM for self-diffusion of PIB ($M = 2.47 \times 10^5$) in chains of the same length (○), in 1.1×10^6 (●), in 1.9×10^6 (△), and in 4.9×10^6 (▲).

accords with the observation of Deschamps and Léger[40] that the predicted reptation exponent is only obtained when the matrix chains are "frozen" on the time scale of the probe motions.

It has been previously demonstrated[29-31] that, in a certain range, the molecular weight of the matrix has an influence on the probe diffusion rate. This enhancement of the diffusion rate of the probe with decreasing matrix MW was considered to arise from contributions of the motions of the matrix chains, which serve to continually relax the local constraints to probe diffusion (so-called "constraint release"). According to Kim et al.,[31] only when the molecular weight of the matrix exceeds that of the probe by a factor of 3–5 does this dependence disappear,[31] as would be anticipated for "pure" reptation (Figure 15).

Figure 16 shows a double logarithmic plot of D_{probe} versus CM for $M = 2.47 \times 10^5$ in different MW matrix solutions, as well as in solutions of the same MW. These data contradict the reptation model, which assumes independence of the matrix MW. It may be noted that Skolnick et al.[34] predict a matrix MW exponent of −1 in bidisperse melts. A dependence on M_m^{-1} is equivalent to normalization of the matrix concentration with the entanglement concentration.[42] This result may be contrasted with that observed by Kim et al.[31] who found D_{probe} to be independent of matrix MW for higher values of M_{matrix}. When the probe size is very much smaller than the average mesh size of the matrix, it is clear that the probe diffusion must become independent of M_{matrix}, although in this limit the probe chain will not be constrained to reptate.

Figure 17A compares the pronounced difference in the concentration dependence of the product $(D_{probe}\eta)$ when $M_{probe} \gg M_{matrix}$ and the reverse case when $M_{probe} \ll$

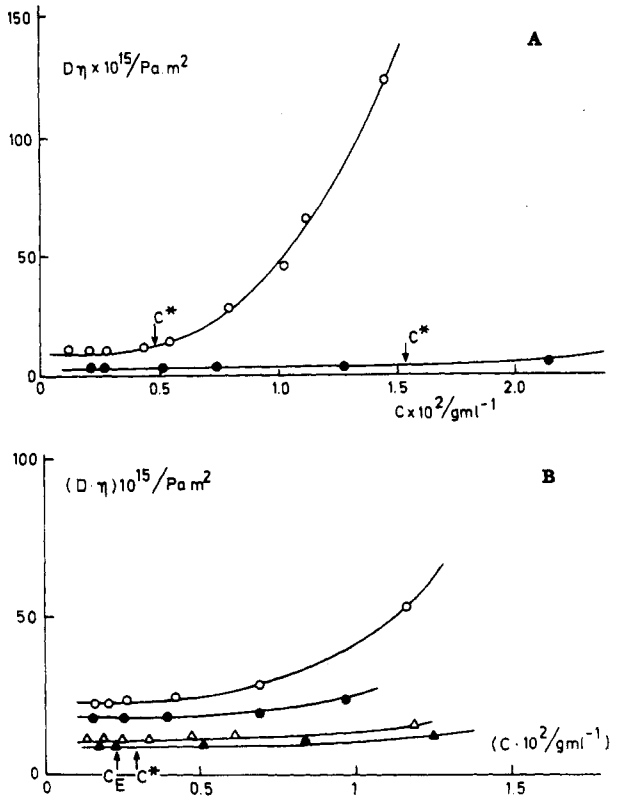

Figure 17. (A) Dependence of $(D\eta)$ on concentration where D is the probe diffusion coefficient and η the macroscopic viscosity of the PIB solution. PIB (2.47×10^5) in 1.9×10^6 (○); PIB (4.9×10^6) in 2.47×10^5 (●). C^* is shown for the matrix. (B) Concentration dependence of $(D\eta)$ for different MW samples of PIB in matrix polymer $M = 4.9 \times 10^6$. Probe $M = 1.82 \times 10^5$ (○); $M = 2.47 \times 10^5$ (●); $M = 6.1 \times 10^5$ (△); $M = 8.56 \times 10^5$ (▲).

M_{matrix}. In the former, $D\eta \approx$ constant (i.e., Stokes–Einstein diffusion) and the matrix chains are not entangled over the concentration range used. With the latter inequality, however, $(D\eta)$ increases strongly with matrix concentration after an initial plateau up to the vicinity of C^* (and the nearly coincident value of the entanglement concentration $C_E \simeq 0.6\%$), which is described by S–E diffusion. Above C^* the diffusion of small probe coils is clearly not determined by the macroscopic viscosity. We note that Martin[41] has interpreted the strong positive curvature in similar $D\eta$ plots for the polystyrene/poly(vinyl methyl ether) system to represent a crossover from S–E diffusion to reptation. This is not the only interpretation. The viscosity of the matrix will increase rapidly above C_E and may not correspondingly retard diffusion of probe chains having a size of the same order or smaller than the average mesh size. Thus, with decreasing probe size, one anticipates $D\eta$ to increase more strongly with increasing concentration as is observed; see, for example, Figure 17B. The curvature increases as probe MW decreases, reflecting the diminishing friction of the entangled matrix on successively smaller probe chains. For short chains R_g is of the same order as the "blob" size of the matrix, and it is then doubtful whether the probe chains would be constrained to reptate by the matrix.

Similar data to those shown in Figure 12 were obtained using molecular weight probes having $M = 1.82 \times 10^5$, 6.1×10^5, and 8.56×10^5. The crossover on the time scale of the relative peak positions of probe and matrix components, as demonstrated in Figure 13, applies in each case. The concentration dependences for these fractions covering the dilute–semidilute crossover region are shown in Figure 18. What is observed is, within experimental error, a

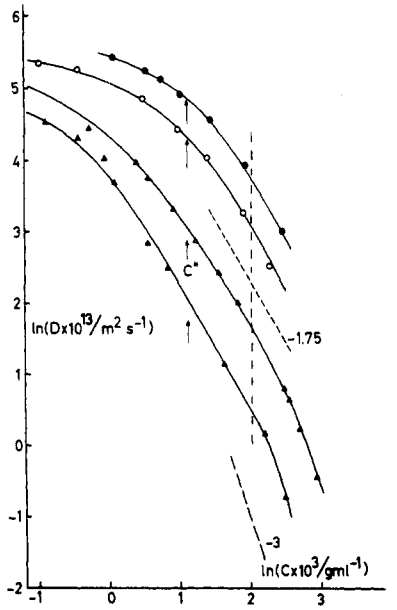

Figure 18. Logarithmic diagram for probe diffusion coefficients and matrix ($M = 4.9 \times 10^6$) concentration. Probe molecular weights are the following: 1.82×10^5 (●); 2.47×10^5 (○); 6.1×10^5 (△); 8.56×10^5 (▲). C^* for the matrix is indicated[37] as are the theoretical slopes for a good solvent (−1.75) and a Θ solvent (−3). The vertical dotted line indicates where the molecular weight dependence shown in Figure 19 has been estimated.

smooth and continuous increase in slope. Over a restricted concentration range, however, the slope is not inconsistent with the value of −1.75 predicted theoretically in thermodynamically good solvents,[25] (indicated by the broken line), a conclusion which is in harmony with that of other workers who have measured a self-diffusion in the binary systems using, for example, PFG NMR[31,32] and forced Rayleigh scattering (FRS).[33] Since, however, the uncertainty in the value of D lies at best at ±3% with any of the methods, it is not possible to unequivocally decide between continuous curvature and the postulated slopes and considerable ambiguity remains concerning the transport mechanism. The present data do not extend to sufficiently high concentrations for a meaningful discussion of a possible limiting value of the slope. The observed curvature has been shown by other groups[31-33] to increase smoothly with concentration toward a tangent of −3,[25] which could be interpreted to mean that the probe coil had contracted to its Θ dimensions. There is an indication that this could be so in the highest concentration range covered with the fractions of $M = 6.1 \times 10^5$ and $M = 8.56 \times 10^5$ as shown in the diagram.

von Meerwall et al.[32] have discussed the effect of the concentration dependence of the monomeric friction coefficient on the apparent exponent and show that it leads to an enhanced slope at the high concentration end, which may greatly exceed the value of −3, the maximum predicted by scaling laws. However, this effect (which may be simply taken into account[32]) should first become important at a matrix concentration in the vicinity of 10–15%. We have selected a concentration range for the matrix polymer with a maximum of about 1% in order to eliminate this complication.

The molecular weight dependence of the probe diffusion coefficient shown in Figure 19 (taken at a concentration of $C = 0.074$ g mL^1 as indicated in Figure 18) does not contradict the slope of −2, which is the value anticipated from theory.[25] (However, Kim et al.[31] found M^{-3} at the highest MW's, an exponent for which there is no theoretical support.) For probes with $M = 1.82 \times 10^5$ and 2.47

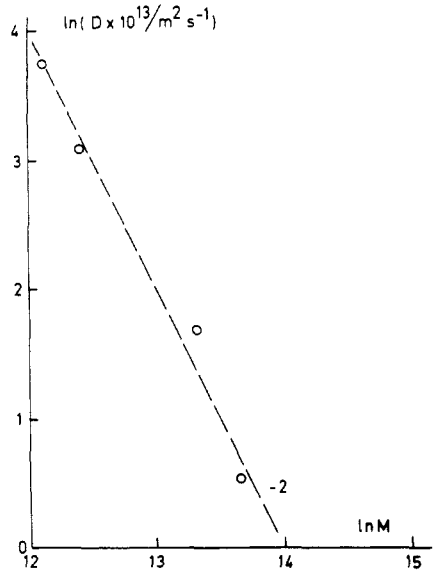

Figure 19. Molecular weight dependence; see text to Figure 18.

$\times 10^5$, the relaxation times are shorter than the disentanglement time of the matrix (T_R) estimated using eq 2, so that the elastic properties of the transient gel are retained and reptation would be anticipated as the preferred mechanism for translation. However, for the probes with $M = 6.1 \times 10^5$ and $M = 8.56 \times 10^5$, $(\tau)_{probe} > (T_R)_{matrix}$ so that the matrix constitutes a viscous medium for diffusion of the probe chain. The same overall form of the curves in Figure 18 is observed, which may suggest a common transport mechanism for probe chains of different sizes in an increasingly congested system as entanglements develop in the matrix.

As discussed previously, the MW exponent of −2 does not in itself demonstrate that a reptative mechanism is valid; for example, Skolnick and co-workers[34] in simulation experiments, find the M^{-2} dependence for probe diffusion in congested systems without resorting to the "tube" model.[26] They concluded that the lateral fluctuations of the confining chains are such that the probe chains may diffuse without following the motion of the matrix chains. Also, from comparisons between data for the self-diffusion of polymers and globular proteins, Phillies[44] concluded that reptation is not the underlying mechanism of self-diffusion in solution. Phillies derived a stretched exponential equation that provides a good fit to the self-diffusion data in the literature for a wide range of particles at both dilute and semidilute solution concentrations.

The emphasis here, however, is not to establish a mechanism by which diffusion proceeds nor precise values for the concentration and MW exponents but rather to demonstrate that self-diffusion of the chemically identical components in ternary systems can be measured with a useful degree of precision using DLS.

A "slow mode" was featured in DLS literature dealing with semidilute solutions of binary blends.[35] However, in contrast to the present results, their value of D_{slow} was considerably lower than the self-diffusion coefficients (determined using forced Rayleigh scattering). Thus, one may conclude that the movement of clusters of chains in the semidilute matrix is responsible for the slow concentration fluctuations in that case. This conclusion was also reached concerning the slow mode earlier observed in binary semidilute solutions.[36] Due to the resultant size polydispersity, a slow mode corresponding to self-diffusion of the clusters will be observed. This explains both the observed agreement with scaling relationships for self-

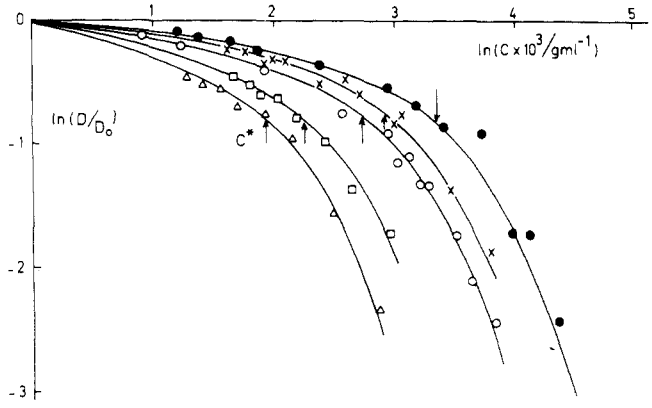

Figure 20. Data analogous to those in Figure 7 but for a polystyrene fraction as probe ($M = 8 \times 10^6$). The same PIB fractions have been used as matrix.

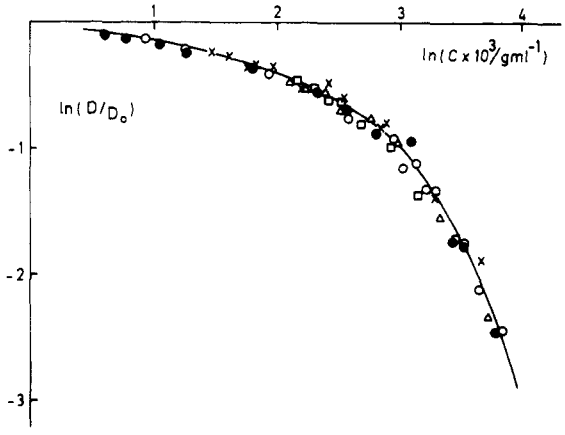

Figure 21. Data in Figure 20 but with matrix concentration normalized using the overlap concentration, C^*.

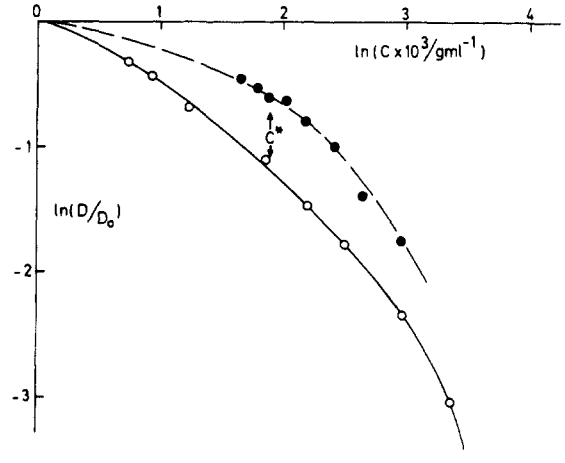

Figure 22. Comparison between the reduced diffusion coefficients for (i) PS (8×10^6) (●) and (ii) PIB 4.9×10^6 (○), both in solutions of PIB (6.1×10^5) as the matrix to illustrate the influence of limited polymer compatibility. The matrix polymer overlap concentration is indicated.

diffusion as well as the misfit with single-coil self-diffusion coefficients.

3. Polystyrene/Polyisobutylene/Chloroform. The self-diffusion of large PS coils ($M = 8 \times 10^6$) in solutions of PIB of lower molecular weight was examined. Figure 20 shows the $(D/D_0)_{PS}$ versus C_{PIB} log–log diagrams and Figure 21 with the PIB concentrations normalized by C^* for the PIB matrix.

Figure 22 compares data for PIB(4.9×10^6)/PIB(6.1×10^5) with the corresponding data for PS(8×10^6)/PIB($M = 6.1 \times 10^5$). The larger normalized diffusion coefficient,

D/D_0, for the PS probe at a given value of C_{PIB} shows that the PS coil is significantly more contracted than the PIB coil at the same PIB matrix concentration (and which had been shown in Figure 9 to be identical with the curve for the SiO_2 spheres). This is an expected result since PS and PIB chains are known to be imcompatible; see, for example, Nagata et al.[45] This finding is also in line with the results of Lodge et al.[5] for PS chains in poly(vinyl methyl ether) solutions who concluded that the PS chains contract to the Θ dimension already at very low concentrations of PVME.

Conclusions

Two relaxation processes are observed in solutions of two monodisperse polymers, one of which is semidilute, identical except in molecular weight. This arises from the modulation of the signal for the one polymer chain due to the presence of the second, as described by Benmouna et al.[16,17] With a trace amount of one component (the probe chain), its self-diffusion coefficient may be determined in addition to the cooperative diffusion coefficient of the semidilute matrix polymer.

The self-diffusion of a high MW coil in semidilute solutions of a lower MW component approximately follows the Stokes–Einstein mechanism, as is also the case for hard spheres in the same system; the reduced self-diffusion coefficients (D/D_0) for the coil and sphere are experimentally indistinguishable. Above the overlap concentration of the matrix, there is apparently an increasing coupling of the motions of probe and matrix chains (both for the coil and the hard sphere) and no evidence that that the coil deswells with increasing matrix concentration.

Transport of a low MW probe in semidilute solutions of the high MW component is not inconsistent, over a limited range of concentration, with scaling predictions for self-diffusion in congested systems; viz, $D \sim M^{-2}C^{-1.75}$ in a good solvent. At higher concentration, there is a smooth increase in curvature toward a possible limiting slope of −3 for the concentration exponent. However, within experimental error, the data are also well-represented by a smooth curve over the whole range of concentration and thus reptation cannot be said to have been established. A mechanism in which diffusional mobility is determined by the increasing congestion as the entanglement density in the matrix increases[34] is seen to be as plausible as reptation. This conclusion supports that of Phillies[44] who questions the relevance of the reptation mechanism for polymers in solution.

Acknowledgment. We thank Drs. C. Koňák and P. Stěpánek, Prague, for stimulating discussions. This work was supported by the Swedish Natural Science Research Council and the Swedish National Board for Technical Development. Z.P. thanks 1959 Års fund for a stipendium.

Registry No. PIB, 9003-27-4; PS, 9003-53-6.

References and Notes

(1) Lodge, T. P. *Macromolecules* **1983**, *16*, 1393; **1986**, *19*, 2986.
(2) Martin, J. E. *Macromolecules* **1984**, *17*, 1279; **1986**, *19*, 922.
(3) Nemoto, N.; Inoue, T.; Makita, Y.; Tsunashima, Y.; Kurata, M. *Macromolecules* **1985**, *18*, 2516.
(4) Wheeler, L. M.; Lodge, T. P.; Hanley, B.; Tirrell, M. *Macromolecules* **1987**, *20*, 1120.
(5) Lodge, T. P.; Wheeler, L. M. *Macromolecules* **1986**, *19*, 2983.
(6) Numasawa, N.; Kuwamoto, K.; Nose, T. *Macromolecules* **1986**, *19*, 2593.
(7) Chu, B.; Wu, D.-q.; Liang, G.-M. *Macromolecules* **1986**, *19*, 2665.
(8) Chu, B.; Wu, D.-q. *Macromolecules* **1987**, *20*, 1606.
(9) Brown, W.; Rymdén, R. *Macromolecules* **1988**, *21*, 840.
(10) Zhou, P.; Brown, W. *Macromolecules* **1989**, *22*, 890.
(11) Chang, T.; Han, C. C.; Wheeler, L. M.; Lodge, T. P. *Macromolecules* **1988**, *21*, 1870.
(12) Phillies, G. D. J. *J. Chem. Phys.* **1974**, *60*, 983.
(13) Pusey, P. N.; Fijnaut, H. M.; Vrij, A. *J. Chem. Phys.* **1982**, *77*, 4270.
(14) Phillies, G. D. J. *J. Chem. Phys.* **1983**, *79*, 2325.
(15) Joanny, J.-F.; Leibler, L.; Ball, R. *J. Chem. Phys.* **1984**, *81*, 4640.
(16) (a) Benmouna, M.; Benoit, H.; Duval, M.; Akcasu, Z. *Macromolecules* **1987**, *20*, 1107. (b) Borsali, R.; Duval, M.; Benoit, H.; Benmouna, M. *Macromolecules* **1987**, *20*, 1112.
(17) Borsali, R.; Duval, M.; Benmouna, M. *Macromolecules* **1989**, *22*, 816.
(18) Jakeš, J., to be published.
(19) Provencher, S. W. *Makromol. Chem.* **1979**, *180*, 201.
(20) Livesey, A. K.; Licinio, P.; Delaye, M. *J. Chem. Phys.* **1986**, *84*, 5102.
(21) Licinio, P.; Delaye, M.; Livesey, A. K.; Léger, L. *J. Phys. (Paris)* **1987**, *48*, 1217.
(22) Vrij, A.; Jansen, J. W.; Dhont, J. K. G.; Pathmamanoharan, C.; Kops-Werkhoven, M. M.; Fijnaut, H. M. *Faraday Discuss. Chem. Soc.* **1983**, *76*, 19.
(23) Stilbs, P. *J. Colloid Int. Sci* **1982**, *87*, 385.
(24) Brown, W.; Stepanek, P. *Macromolecules* **1988**, *21*, 1791.
(25) de Gennes, P. G. *Scaling Concepts in Polymer Physics*; Cornell University Press: London, 1979.
(26) Doi, M.; Edwards, S. F. *The Theory of Polymer Dynamics*; Clarendon: Oxford, 1986.
(27) Reina, J. C.; Bansil, R.; Konak, C., submitted for publication in *Macromolecules*.
(28) Joanny, J. F.; Grant, P.; Turkevich, L. A.; Pincus, P. *J. Phys. (Paris)* **1981**, *42*, 1045.
(29) Léger, L. In *Polymer Motion in Dense Systems*; Richter, D., Springer, T., Eds.; Springer: Berlin, 1988; vol. 29.
(30) Marmonier, M. F.; Léger, L. *Phys. Rev. Lett.* **1985**, *55*, 1078.
(31) Kim, H.; Chang, T.; Yohanan, J. M.; Wang, L.; Yu, H. *Macromolecules* **1986**, *19*, 2737.
(32) von Meerwall, E. D.; Amis, E. J.; Ferry, J. D. *Macromolecules* **1985**, *18*, 260.
(33) Wesson, J. A.; Noh, I.; Kitano, T.; Yu, H. *Macromolecules* **1984**, *17*, 782.
(34) Kolinski, A.; Skolnick, J.; Varis, R. *J. Chem. Phys.* **1987**, *86*, 1567; **1987**, *86*, 7164; **1987**, *86*, 7174. Skolnick, J.; Yaris, R.; Kolinski, A. *J. Chem. Phys.* **1988**, *88*, 1407; Skolnick, J.; Yaris, R. *J. Chem. Phys.* **1988**, *88*, 1418.
(35) Nemoto, N.; Makita, Y.; Tsunashima, Y.; Kurata, M. *Macromolecules* **1984**, *17*, 2629.
(36) Brown, W. *Macromolecules* **1984**, *17*, 66.
(37) $C^* \approx 3M/4\pi R_g^3 N_A \approx [\eta]^{-1}$.
(38) Brown, W. *Polymer* **1984**, *25*, 680.
(39) Nemoto, N.; Okada, S.; Inoue, T.; Kurata, M. *Macromolecules* **1988**, *21*, 1502, 1509.
(40) Deschamps, H.; Léger, L. *Macromolecules* **1986**, *19*, 2760.
(41) Martin, J. E. *Macromolecules* **1984**, *17*, 1279; **1986**, *19*, 922.
(42) $C_E \approx \rho M_E/M$ where ρ is the density of polymer, MW = M, and M_E is the MW between entanglements (=8600 for PIB).[43]
(43) Ferry, J. D. *Viscoelastic Properties of Polymers*; Wiley: New York, 1980.
(44) Phillies, G. D. J. *Macromolecules* **1986**, *19*, 2367; **1987**, *20*, 558.
(45) Nagata, M.; Fukuda, T.; Inagaki, H. *Macromolecules* **1987**, *20*, 2173.